

PARTICLES AND FIELDS • OPEN ACCESS

Measurement of integrated luminosity and center-of-mass energy of data taken by BESIII at $\sqrt{s}=2.125$ GeV

To cite this article: M. Ablikim *et al* 2017 *Chinese Phys. C* **41** 113001

View the [article online](#) for updates and enhancements.

Related content

- [Measurement of e+ e- DD cross sections at the \(3770\) resonance](#)
M. Ablikim, M. N. Achasov, S. Ahmed et al.
- [Measurement of the integrated Luminosities of cross-section scan data samples around the \$\psi\(3770\)\$ mass region](#)
M. Ablikim, M. N. Achasov, S. Ahmed et al.
- [Luminosity measurements for the R scan experiment at BESIII](#)
M. Ablikim, M. N. Achasov, S. Ahmed et al.

Recent citations

- [Search for a strangeonium-like structure \$Z_s\$ decaying into \$\psi\$ and a measurement of the cross section e+e-](#)
M. Ablikim *et al*

Measurement of integrated luminosity and center-of-mass energy of data taken by BESIII at $\sqrt{s}=2.125$ GeV*

M. Ablikim(麦迪娜)¹ M. N. Achasov^{9,e} S. Ahmed¹⁴ X. C. Ai(艾小聪)¹ O. Albayrak⁵ M. Albrecht⁴ D. J. Ambrose⁴⁴ A. Amoroso^{49A,49C} F. F. An(安芬芬)¹ Q. An(安琪)^{46,a} J. Z. Bai(白景芝)¹ R. Baldini Ferroli^{20A} Y. Ban(班勇)³¹ D. W. Bennett¹⁹ J. V. Bennett⁵ N. Berger²² M. Bertani^{20A} D. Bettoni^{21A} J. M. Bian(边渐鸣)⁴³ F. Bianchi^{49A,49C} E. Boger^{23,c} I. Boyko²³ R. A. Briere⁵ H. Cai(蔡浩)⁵¹ X. Cai(蔡啸)^{1,a} O. Cakir^{40A} A. Calcaterra^{20A} G. F. Cao(曹国富)¹ S. A. Cetin^{40B} J. Chai^{49C} J. F. Chang(常劭帆)^{1,a} G. Chelkov^{23,c,d} G. Chen(陈刚)¹ H. S. Chen(陈和生)¹ J. C. Chen(陈江川)¹ M. L. Chen(陈玛丽)^{1,a} S. Chen(陈实)⁴¹ S. J. Chen(陈申见)²⁹ X. Chen(谌炫)^{1,a} X. R. Chen(陈旭荣)²⁶ Y. B. Chen(陈元柏)^{1,a} H. P. Cheng(程和平)¹⁷ X. K. Chu(褚新坤)³¹ G. Cibinetto^{21A} H. L. Dai(代洪亮)^{1,a} J. P. Dai(代建平)³⁴ A. Dbeyssi¹⁴ D. Dedovich²³ Z. Y. Deng(邓子艳)¹ A. Denig²² I. Denysenko²³ M. Destefanis^{49A,49C} F. De Mori^{49A,49C} Y. Ding(丁勇)²⁷ C. Dong(董超)³⁰ J. Dong(董静)^{1,a} L. Y. Dong(董燎原)¹ M. Y. Dong(董明义)^{1,a} Z. L. Dou(豆正磊)²⁹ S. X. Du(杜书先)⁵³ P. F. Duan(段鹏飞)¹ J. Z. Fan(范荆州)³⁹ J. Fang(方建)^{1,a} S. S. Fang(房双世)¹ X. Fang(方馨)^{46,a} Y. Fang(方易)¹ R. Farinelli^{21A,21B} L. Fava^{49B,49C} O. Fedorov²³ F. Feldbauer²² G. Felici^{20A} C. Q. Feng(封常青)^{46,a} E. Fioravanti^{21A} M. Fritsch^{14,22} C. D. Fu(傅成栋)¹ Q. Gao(高清)¹ X. L. Gao(高鑫磊)^{46,a} Y. Gao(高原宁)³⁹ Z. Gao(高榛)^{46,a} I. Garzia^{21A} K. Goetzen¹⁰ L. Gong(龚丽)³⁰ W. X. Gong(龚文焯)^{1,a} W. Gradl²² M. Greco^{49A,49C} M. H. Gu(顾旻皓)^{1,a} Y. T. Gu(顾运厅)¹² Y. H. Guan(管颖慧)¹ A. Q. Guo(郭爱强)¹ L. B. Guo(郭立波)²⁸ R. P. Guo(郭如盼)¹ Y. Guo(郭玥)¹ Y. P. Guo(郭玉萍)²² Z. Haddadi²⁵ A. Hafner²² S. Han(韩爽)⁵¹ X. Q. Hao(郝喜庆)¹⁵ F. A. Harris⁴² K. L. He(何康林)¹ F. H. Heinsius⁴ T. Held⁴ Y. K. Heng(衡月昆)^{1,a} T. Holtmann⁴ Z. L. Hou(侯治龙)¹ C. Hu(胡琛)²⁸ H. M. Hu(胡海明)¹ J. F. Hu(胡继峰)^{49A,49C} T. Hu(胡涛)^{1,a} Y. Hu(胡誉)¹ G. S. Huang(黄光顺)^{46,a} J. S. Huang(黄金书)¹⁵ X. T. Huang(黄性涛)³³ X. Z. Huang(黄晓忠)²⁹ Y. Huang(黄勇)²⁹ Z. L. Huang(黄智玲)²⁷ T. Hussain⁴⁸ Q. Ji(纪全)¹ Q. P. Ji(姬清平)¹⁵ X. B. Ji(季晓斌)¹ X. L. Ji(季筱璐)^{1,a} L. W. Jiang(姜鲁文)⁵¹ X. S. Jiang(江晓山)^{1,a} X. Y. Jiang(蒋兴雨)³⁰ J. B. Jiao(焦健斌)³³ Z. Jiao(焦铮)¹⁷ D. P. Jin(金大鹏)^{1,a} S. Jin(金山)¹ T. Johansson⁵⁰ A. Julin⁴³ N. Kalantar-Nayestanaki²⁵ X. L. Kang(康晓琳)¹ X. S. Kang(康晓坤)³⁰ M. Kavatsyuk²⁵ B. C. Ke(柯百谦)⁵ P. Kiese²² R. Kliemt¹⁴ B. Kloss²² O. B. Kolcu^{40B,h} B. Kopf⁴ M. S. Korner⁴² A. Kupsc⁵⁰ W. Kühn²⁴ J. S. Lange²⁴ M. Lara¹⁹ P. Larin¹⁴ H. Leithoff²² C. Leng^{49C} C. Li(李翠)⁵⁰ Cheng Li(李澄)^{46,a} D. M. Li(李德民)⁵³ F. Li(李飞)^{1,a} F. Y. Li(李峰云)³¹ G. Li(李刚)¹ H. B. Li(李海波)¹ H. J. Li(李惠静)¹ J. C. Li(李家才)¹ Jin Li(李瑾)³² K. Li(李康)¹³ K. Li(李科)³³ Lei Li(李蕾)³ P. R. Li(李培荣)⁴¹ Q. Y. Li(李启云)³³ T. Li(李腾)³³ W. D. Li(李卫东)¹ W. G. Li(李卫国)¹ X. L. Li(李晓玲)³³ X. N. Li(李小明)^{1,a} X. Q. Li(李学潜)³⁰ Y. B. Li(李郁博)² Z. B. Li(李志兵)³⁸ H. Liang(梁昊)^{46,a} Y. F. Liang(梁勇飞)³⁶ Y. T. Liang(梁羽铁)²⁴ G. R. Liao(廖广睿)¹¹ D. X. Lin(林德旭)¹⁴ B. Liu(刘冰)³⁴ B. J. Liu(刘北江)¹ C. X. Liu(刘春秀)¹ D. Liu(刘栋)^{46,a} F. H. Liu(刘福虎)³⁵ Fang Liu(刘芳)¹ Feng Liu(刘峰)⁶ H. B. Liu(刘宏邦)¹² H. H. Liu(刘汇慧)¹⁶ H. H. Liu(刘欢欢)¹ H. M. Liu(刘怀民)¹ J. Liu(刘杰)¹ J. B. Liu(刘建北)^{46,a} J. P. Liu(刘觉平)⁵¹ J. Y. Liu(刘晶译)¹ K. Liu(刘凯)³⁹ K. Y. Liu(刘魁勇)²⁷ L. D. Liu(刘兰雕)³¹ P. L. Liu(刘佩莲)^{1,a} Q. Liu(刘倩)⁴¹ S. B. Liu(刘树彬)^{46,a} X. Liu(刘翔)²⁶ Y. B. Liu(刘玉斌)³⁰ Y. Y. Liu(刘媛媛)³⁰ Z. A. Liu(刘振安)^{1,a} Zhiqing Liu(刘智青)²² H. Loehner²⁵ Y. F. Long(龙云飞)³¹ X. C. Lou(娄辛丑)^{1,a,g} H. J. Lu(吕海江)¹⁷ J. G. Lu(吕军光)^{1,a} Y. Lu(卢宇)¹ Y. P. Lu(卢宇鹏)^{1,a} C. L. Luo(罗成林)²⁸ M. X. Luo(罗民兴)⁵² T. Luo⁴² X. L. Luo(罗小兰)^{1,a} X. R. Lyu(吕晓睿)⁴¹ F. C. Ma(马凤才)²⁷ H. L. Ma(马海龙)¹ L. L. Ma(马连良)³³ M. M. Ma(马明明)¹ Q. M. Ma(马秋梅)¹ T. Ma(马天)¹ X. N. Ma(马旭宁)³⁰ X. Y. Ma(马晓娟)^{1,a} Y. M. Ma(马玉明)³³ F. E. Maas¹⁴ M. Maggiora^{49A,49C} Q. A. Malik⁴⁸ Y. J. Mao(冒亚军)³¹ Z. P. Mao(毛泽普)¹ S. Marcello^{49A,49C} J. G. Messchendorp²⁵ G. Mezzadri^{21B} J. Min(闵建)^{1,a} T. J. Min(闵天觉)¹ R. E. Mitchell¹⁹ X. H. Mo(莫晓虎)^{1,a} Y. J. Mo(莫玉俊)⁶ C. Morales Morales¹⁴ N. Yu. Muchnoi^{9,e} H. Muramatsu⁴³ P. Musiol⁴ Y. Nefedov²³ F. Nerling¹⁴ I. B. Nikolaev^{9,e}

Received 1 June 2017

* Supported in part by National Key Basic Research Program of China (2015CB856700), National Natural Science Foundation of China (NSFC) (11235011, 11322544, 11335008, 11425524, 11635010, 11675184, 11735014), the Chinese Academy of Sciences (CAS) Large-Scale Scientific Facility Program; the CAS Center for Excellence in Particle Physics (CCEPP); the Collaborative Innovation Center for Particles and Interactions (CICPI); Joint Large-Scale Scientific Facility Funds of the NSFC and CAS (U1232201, U1332201, U1532257, U1532258), CAS (KJCX2-YW-N29, KJCX2-YW-N45), 100 Talents Program of CAS; National 1000 Talents Program of China; INPAC and Shanghai Key Laboratory for Particle Physics and Cosmology; German Research Foundation DFG (Collaborative Research Center CRC 1044, FOR 2359), Istituto Nazionale di Fisica Nucleare, Italy; Koninklijke Nederlandse Akademie van Wetenschappen (KNAW) (530-4CDP03), Ministry of Development of Turkey (DPT2006K-120470), National Natural Science Foundation of China (NSFC) (11505010), The Swedish Research Council; U. S. Department of Energy (DE-FG02-05ER41374, DE-SC-0010118, DE-SC-0010504, DE-SC-0012069), U.S. National Science Foundation; University of Groningen (RuG) and the Helmholtzzentrum fuer Schwerionenforschung GmbH (GSI), Darmstadt; WCU Program of National Research Foundation of Korea (R32-2008-000-10155-0)



Content from this work may be used under the terms of the Creative Commons Attribution 3.0 licence. Any further distribution of this work must maintain attribution to the author(s) and the title of the work, journal citation and DOI. Article funded by SCOAP³ and published under licence by Chinese Physical Society and the Institute of High Energy Physics of the Chinese Academy of Sciences and the Institute of Modern Physics of the Chinese Academy of Sciences and IOP Publishing Ltd

Z. Ning(宁哲)^{1,a} S. Nisar⁸ S. L. Niu(牛顺利)^{1,a} X. Y. Niu(牛讯伊)¹ S. L. Olsen(馬鵬)³² Q. Ouyang(欧阳群)^{1,a} S. Pacetti^{20B}
 Y. Pan(潘越)^{46,a} P. Patteri^{20A} M. Pelizaeus⁴ H. P. Peng(彭海平)^{46,a} K. Peters^{10,i} J. Pettersson⁵⁰ J. L. Ping(平加伦)²⁸
 R. G. Ping(平荣刚)¹ R. Poling⁴³ V. Prasad¹ H. R. Qi(漆红荣)² M. Qi(祁鸣)²⁹ S. Qian(钱森)^{1,a} C. F. Qiao(乔从丰)⁴¹
 L. Q. Qin(秦丽清)³³ N. Qin(覃拈)⁵¹ X. S. Qin(秦小帅)¹ Z. H. Qin(秦中华)^{1,a} J. F. Qiu(邱进发)¹ K. H. Rashid⁴⁸
 C. F. Redmer²² M. Ripka²² G. Rong(荣刚)¹ Ch. Rosner¹⁴ X. D. Ruan(阮向东)¹² A. Sarantsev^{23,f} M. Savrié^{21B} C. Schmier⁴
 K. Schoenning⁵⁰ S. Schumann²² W. Shan(单葳)³¹ M. Shao(邵明)^{46,a} C. P. Shen(沈成平)² P. X. Shen(沈培迅)³⁰ X. Y. Shen(沈
 肖雁)¹ H. Y. Sheng(盛华义)¹ M. Shi(施萌)¹ W. M. Song(宋维民)¹ X. Y. Song(宋欣颖)¹ S. Sosio^{49A,49C} S. Spataro^{49A,49C}
 G. X. Sun(孙功星)¹ J. F. Sun(孙俊峰)¹⁵ S. S. Sun(孙胜森)¹ X. H. Sun(孙新华)¹ Y. J. Sun(孙勇杰)^{46,a} Y. Z. Sun(孙永昭)¹
 Z. J. Sun(孙志嘉)^{1,a} Z. T. Sun(孙振田)¹⁹ C. J. Tang(唐昌建)³⁶ X. Tang(唐晓)¹ I. Tapan^{40C} E. H. Thorndike⁴⁴ M. Tiemens²⁵
 I. Uman^{40D} G. S. Varner⁴² B. Wang(王斌)³⁰ B. L. Wang(王滨龙)⁴¹ D. Wang(王东)³¹ D. Y. Wang(王大勇)³¹ K. Wang(王
 科)^{1,a} L. L. Wang(王亮亮)¹ L. S. Wang(王灵淑)¹ M. Wang(王萌)³³ P. Wang(王平)¹ P. L. Wang(王佩良)¹ W. Wang(王炜)^{1,a}
 W. P. Wang(王维平)^{46,a} X. F. Wang(王雄飞)³⁹ Y. Wang(王越)³⁷ Y. D. Wang(王雅迪)¹⁴ Y. F. Wang(王贻芳)^{1,a}
 Y. Q. Wang(王亚乾)²² Z. Wang(王铮)^{1,a} Z. G. Wang(王志刚)^{1,a} Z. H. Wang(王志宏)^{46,a} Z. Y. Wang(王至勇)¹ Z. Y. Wang(王
 宗源)¹ T. Weber²² D. H. Wei(魏代会)¹¹ P. Weidenkaff²² S. P. Wen(文硕频)¹ U. Wiedner⁴ M. Wolke⁵⁰ L. H. Wu(伍灵慧)¹
 L. J. Wu(吴连近)¹ Z. Wu(吴智)^{1,a} L. Xia(夏磊)^{46,a} L. G. Xia(夏力钢)³⁹ Y. Xia(夏宇)¹⁸ D. Xiao(肖栋)¹ H. Xiao(肖浩)⁴⁷
 Z. J. Xiao(肖振宇)²⁸ Y. G. Xie(谢宇广)^{1,a} Q. L. Xiu(修青磊)^{1,a} G. F. Xu(许国发)¹ J. J. Xu(徐静静)¹ L. Xu(徐雷)¹
 Q. J. Xu(徐庆君)¹³ Q. N. Xu(徐庆年)⁴¹ X. P. Xu(徐新平)³⁷ L. Yan(严亮)^{49A,49C} W. B. Yan(鄢文标)^{46,a} W. C. Yan(闫文
 成)^{46,a} Y. H. Yan(颜永红)¹⁸ H. J. Yang(杨海军)³⁴ H. X. Yang(杨洪勋)¹ L. Yang(杨柳)⁵¹ Y. X. Yang(杨永栩)¹¹ M. Ye(叶
 梅)^{1,a} M. H. Ye(叶铭汉)⁷ J. H. Yin(殷俊昊)¹ Z. Y. You(尤郑响)³⁸ B. X. Yu(俞伯祥)^{1,a} C. X. Yu(喻纯旭)³⁰ J. S. Yu(俞洁
 晟)²⁶ C. Z. Yuan(苑长征)¹ W. L. Yuan(袁文龙)²⁹ Y. Yuan(袁野)¹ A. Yuncu^{40B,b} A. A. Zafar⁴⁸ A. Zallo^{20A} Y. Zeng(曾云)¹⁸
 Z. Zeng(曾哲)^{46,a} B. X. Zhang(张丙新)¹ B. Y. Zhang(张炳云)^{1,a} C. Zhang(张驰)²⁹ C. C. Zhang(张长春)¹ D. H. Zhang(张达
 华)¹ H. H. Zhang(张宏浩)³⁸ H. Y. Zhang(章红宇)^{1,a} J. Zhang(张晋)¹ J. J. Zhang(张佳佳)¹ J. L. Zhang(张杰磊)¹
 J. Q. Zhang(张敬庆)¹ J. W. Zhang(张家文)^{1,a} J. Y. Zhang(张建勇)¹ J. Z. Zhang(张景芝)¹ K. Zhang(张坤)¹ L. Zhang(张磊)¹
 S. Q. Zhang(张士权)³⁰ X. Y. Zhang(张学尧)³³ Y. Zhang(张瑶)¹ Y. H. Zhang(张银鸿)^{1,a} Y. N. Zhang(张宇宁)⁴¹
 Y. T. Zhang(张亚腾)^{46,a} Yu Zhang(张宇)⁴¹ Z. H. Zhang(张正好)⁶ Z. P. Zhang(张子平)⁴⁶ Z. Y. Zhang(张振宇)⁵¹ G. Zhao(赵
 光)¹ J. W. Zhao(赵京伟)^{1,a} J. Y. Zhao(赵静宜)¹ J. Z. Zhao(赵京周)^{1,a} Lei Zhao(赵雷)^{46,a} Ling Zhao(赵玲)¹ M. G. Zhao(赵明
 刚)³⁰ Q. Zhao(赵强)¹ Q. W. Zhao(赵庆旺)¹ S. J. Zhao(赵书俊)⁵³ T. C. Zhao(赵天池)¹ Y. B. Zhao(赵豫斌)^{1,a} Z. G. Zhao(赵政
 国)^{46,a} A. Zhemchugov^{23,c} B. Zheng(郑波)⁴⁷ J. P. Zheng(郑建平)^{1,a} W. J. Zheng(郑文静)³³ Y. H. Zheng(郑阳恒)⁴¹
 B. Zhong(钟彬)²⁸ L. Zhou(周莉)^{1,a} X. Zhou(周详)⁵¹ X. K. Zhou(周晓康)^{46,a} X. R. Zhou(周小蓉)^{46,a} X. Y. Zhou(周兴玉)¹
 K. Zhu(朱凯)¹ K. J. Zhu(朱科军)^{1,a} S. Zhu(朱帅)¹ S. H. Zhu(朱世海)⁴⁵ X. L. Zhu(朱相雷)³⁹ Y. C. Zhu(朱莹春)^{46,a}
 Y. S. Zhu(朱永生)¹ Z. A. Zhu(朱自安)¹ J. Zhuang(庄建)^{1,a} L. Zotti^{49A,49C} B. S. Zou(邹冰松)¹ J. H. Zou(邹佳恒)¹

(BESIII Collaboration)

¹ Institute of High Energy Physics, Beijing 100049, China² Beihang University, Beijing 100191, China³ Beijing Institute of Petrochemical Technology, Beijing 102617, China⁴ Bochum Ruhr-University, D-44780 Bochum, Germany⁵ Carnegie Mellon University, Pittsburgh, Pennsylvania 15213, USA⁶ Central China Normal University, Wuhan 430079, China⁷ China Center of Advanced Science and Technology, Beijing 100190, China⁸ COMSATS Institute of Information Technology, Lahore, Defence Road, Off Raiwind Road, 54000 Lahore, Pakistan⁹ G.I. Budker Institute of Nuclear Physics SB RAS (BINP), Novosibirsk 630090, Russia¹⁰ GSI Helmholtzcentre for Heavy Ion Research GmbH, D-64291 Darmstadt, Germany¹¹ Guangxi Normal University, Guilin 541004, China¹² Guangxi University, Nanning 530004, China¹³ Hangzhou Normal University, Hangzhou 310036, China¹⁴ Helmholtz Institute Mainz, Johann-Joachim-Becher-Weg 45, D-55099 Mainz, Germany¹⁵ Henan Normal University, Xinxiang 453007, China¹⁶ Henan University of Science and Technology, Luoyang 471003, China¹⁷ Huangshan College, Huangshan 245000, China¹⁸ Hunan University, Changsha 410082, China¹⁹ Indiana University, Bloomington, Indiana 47405, USA²⁰ (A)INFN Laboratori Nazionali di Frascati, I-00044, Frascati, Italy; (B)INFN and University of Perugia, I-06100, Perugia, Italy²¹ (A)INFN Sezione di Ferrara, I-44122, Ferrara, Italy; (B)University of Ferrara, I-44122, Ferrara, Italy²² Johannes Gutenberg University of Mainz, Johann-Joachim-Becher-Weg 45, D-55099 Mainz, Germany²³ Joint Institute for Nuclear Research, 141980 Dubna, Moscow region, Russia²⁴ Justus-Liebig-Universitaet Giessen, II. Physikalisches Institut, Heinrich-Buff-Ring 16, D-35392 Giessen, Germany²⁵ KVI-CART, University of Groningen, NL-9747 AA Groningen, The Netherlands

- ²⁶ Lanzhou University, Lanzhou 730000, China
²⁷ Liaoning University, Shenyang 110036, China
²⁸ Nanjing Normal University, Nanjing 210023, China
²⁹ Nanjing University, Nanjing 210093, China
³⁰ Nankai University, Tianjin 300071, China
³¹ Peking University, Beijing 100871, China
³² Seoul National University, Seoul, 151-747 Korea
³³ Shandong University, Jinan 250100, China
³⁴ Shanghai Jiao Tong University, Shanghai 200240, China
³⁵ Shanxi University, Taiyuan 030006, China
³⁶ Sichuan University, Chengdu 610064, China
³⁷ Soochow University, Suzhou 215006, China
³⁸ Sun Yat-Sen University, Guangzhou 510275, China
³⁹ Tsinghua University, Beijing 100084, China
⁴⁰ (A)Ankara University, 06100 Tandogan, Ankara, Turkey; (B)Istanbul Bilgi University, 34060 Eyup, Istanbul, Turkey; (C)Uludag University, 16059 Bursa, Turkey; (D)Near East University, Nicosia, North Cyprus, Mersin 10, Turkey
⁴¹ University of Chinese Academy of Sciences, Beijing 100049, China
⁴² University of Hawaii, Honolulu, Hawaii 96822, USA
⁴³ University of Minnesota, Minneapolis, Minnesota 55455, USA
⁴⁴ University of Rochester, Rochester, New York 14627, USA
⁴⁵ University of Science and Technology Liaoning, Anshan 114051, China
⁴⁶ University of Science and Technology of China, Hefei 230026, China
⁴⁷ University of South China, Hengyang 421001, China
⁴⁸ University of the Punjab, Lahore-54590, Pakistan
⁴⁹ (A)University of Turin, I-10125, Turin, Italy; (B)University of Eastern Piedmont, I-15121, Alessandria, Italy; (C)INFN, I-10125, Turin, Italy
⁵⁰ Uppsala University, Box 516, SE-75120 Uppsala, Sweden
⁵¹ Wuhan University, Wuhan 430072, China
⁵² Zhejiang University, Hangzhou 310027, China
⁵³ Zhengzhou University, Zhengzhou 450001, China
^a Also at State Key Laboratory of Particle Detection and Electronics, Beijing 100049, Hefei 230026, China
^b Also at Bogazici University, 34342 Istanbul, Turkey
^c Also at the Moscow Institute of Physics and Technology, Moscow 141700, Russia
^d Also at the Functional Electronics Laboratory, Tomsk State University, Tomsk, 634050, Russia
^e Also at the Novosibirsk State University, Novosibirsk, 630090, Russia
^f Also at the NRC “Kurchatov Institute”, PNPI, 188300, Gatchina, Russia
^g Also at University of Texas at Dallas, Richardson, Texas 75083, USA
^h Also at Istanbul Arel University, 34295 Istanbul, Turkey
ⁱ Also at Goethe University Frankfurt, 60323 Frankfurt am Main, Germany

Abstract: To study the nature of the state $Y(2175)$, a dedicated data set of e^+e^- collision data was collected at the center-of-mass energy of 2.125 GeV with the BESIII detector at the BEPCII collider. By analyzing large-angle Bhabha scattering events, the integrated luminosity of this data set is determined to be $108.49 \pm 0.02 \pm 0.85 \text{ pb}^{-1}$, where the first uncertainty is statistical and the second one is systematic. In addition, the center-of-mass energy of the data set is determined with radiative dimuon events to be $2126.55 \pm 0.03 \pm 0.85 \text{ MeV}$, where the first uncertainty is statistical and the second one is systematic.

Keywords: Bhabha scattering, luminosity, radiative dimuon events, center-of-mass energy

PACS: 13.66.De, 13.66.Jn **DOI:** 10.1088/1674-1137/41/11/113001

1 Introduction

The state $Y(2175)$, denoted as $\phi(2170)$ in Ref. [1], was first observed by the BaBar experiment [2, 3] in the initial-state-radiation (ISR) process $e^+e^- \rightarrow$

$\gamma_{\text{ISR}}\phi(1020)f_0(980)$, and was subsequently confirmed by BESII [4], Belle [5] and BESIII [6]. The observation of the $Y(2175)$ stimulated many theoretical explanations of its nature, including a $s\bar{s}$ -gluon hybrid [7], an excited ϕ state [8], a tetraquark state [9] and a $\Lambda\bar{\Lambda}$ bound state [10].

To study the $Y(2175)$, a dedicated data set was collected with the BESIII detector [11] at the BEPCII collider in 2015 at the center-of-mass energy (\sqrt{s}) of 2.125 GeV, which is in the vicinity of the peaking cross sections for $e^+e^- \rightarrow \phi\pi\pi$ and $e^+e^- \rightarrow \phi f_0(980)$ decays reported by BaBar [2, 3] and Belle [5].

In this paper, we present a determination of the integrated luminosity of this data set using large-angle Bhabha scattering events $e^+e^- \rightarrow (\gamma)e^+e^-$. A cross check is performed by analyzing di-photon events $e^+e^- \rightarrow \gamma\gamma$. In addition, using the approach described in Ref. [12], we determine the center-of-mass energy using radiative dimuon events $e^+e^- \rightarrow (\gamma)\mu^+\mu^-$, where γ represents possible ISR or FSR (final state radiation) photons.

2 The BESIII detector

BESIII [11] is a general purpose detector, which is located at the BEPCII facility, a double-ring e^+e^- collider with a peak luminosity of $10^{33} \text{ cm}^{-2}\text{s}^{-1}$ at a center-of-mass energy of 3.773 GeV. The BESIII detector covers 93% of the solid angle around the collision point and consists of four main components: 1) A small-cell, helium-based main drift chamber (MDC) with 43 layers providing an average single-hit resolution of 135 μm , and charged-particle momentum resolution in a 1 T magnetic field of 0.5% at 1 GeV/c; 2) A Time-Of-Flight system (TOF) for particle identification composed of a barrel and two end-caps. The barrel has two layers, each consisting of 88 pieces of 5 cm thick, 2.4 m long plastic scintillator. Each end-cap consists of 96 fan-shaped, 5 cm thick, plastic scintillators. The barrel (end-cap) time resolution of 80 ps (110 ps) provides a $2\sigma K/\pi$ separation for momenta up to about 1.0 GeV/c; 3) An electromagnetic calorimeter (EMC) consisting of 6240 CsI(Tl) crystals in a cylindrical structure, arranged in one barrel and two end-caps. The energy resolution for 1.0 GeV photons is 2.5% (5%) in the barrel (end-caps), while the position resolution is 6 mm (9 mm) in the barrel (end-caps); 4) A muon counter (MUC) made of nine layers of resistive plate chambers in the barrel and eight layers in each end-cap, which are incorporated in the iron return yoke of the superconducting magnet. The position resolution is about 2 cm. A GEANT4 [13, 14]-based detector simulation package has been developed to model the detector response.

3 Monte Carlo simulation

In order to determine the detection efficiency and estimate background contributions, one million Monte Carlo (MC) events were simulated at $\sqrt{s}=2.125$ GeV for each of the four processes: $e^+e^- \rightarrow (\gamma)e^+e^-$, $e^+e^- \rightarrow \gamma\gamma$, $e^+e^- \rightarrow (\gamma)\mu^+\mu^-$ and $e^+e^- \rightarrow q\bar{q}$. The first three processes were generated with the Babayaga 3.5 [15] gen-

erator, while $e^+e^- \rightarrow q\bar{q} \rightarrow \text{hadrons}$ was generated with EvtGen [16, 17] according to the ‘LundAreaLaw’ [18, 19].

4 Measurement of the luminosity

4.1 Event selection

To select $e^+e^- \rightarrow (\gamma)e^+e^-$ events, exactly two good tracks with opposite charge were required. Each good charged track was required to pass the interaction point within ± 10 cm in the beam direction ($|V_z| < 10.0$ cm) and within 1.0 cm in the plane perpendicular to the beam ($V_r < 1.0$ cm). Their polar angles θ were required to satisfy $|\cos\theta| < 0.8$ to ensure the tracks were in the barrel part of the detector. The energy deposited in the EMC of each track was required to be greater than $0.65 \times E_{\text{beam}}$, where $E_{\text{beam}} = 2.125/2$ GeV is the beam energy. To select tracks that were back-to-back in the MDC, $|\Delta\theta| \equiv |\theta_1 + \theta_2 - 180^\circ| < 10^\circ$ and $|\Delta\phi| \equiv ||\phi_1 - \phi_2| - 180^\circ| < 5.0^\circ$ were required, where $\theta_{1/2}$ and $\phi_{1/2}$ are the polar and azimuthal angles of the two tracks, respectively. Comparisons between data and MC simulation are shown in Fig. 1.

After applying the above requirements, 33,228,098 events were selected as Bhabha scattering candidates. The background contribution is estimated to be at the level of 10^{-5} using MC samples of $e^+e^- \rightarrow \gamma\gamma$, $e^+e^- \rightarrow (\gamma)\mu^+\mu^-$ and $e^+e^- \rightarrow q\bar{q}$ processes, and is ignored in the calculation of the integrated luminosity. The backgrounds from beam-gas interactions are also ignored due to the powerful rejection rate of the trigger system and the distinguishable features of Bhabha events.

4.2 Integrated luminosity

The integrated luminosity is calculated with

$$L = \frac{N_{\text{obs}}}{\sigma \times \varepsilon \times \varepsilon_{\text{trig}}}, \quad (1)$$

where N_{obs} is the number of observed signal events, σ is the cross section of the specified process, ε is the detection efficiency and $\varepsilon_{\text{trig}}$ is the trigger efficiency.

For the Bhabha scattering process, the cross section at $\sqrt{s}=2.125$ GeV is calculated with the Babayaga generator to be 1621.43 ± 3.47 nb. Using the large sample of MC simulated events, the detection efficiency is determined to be $(18.89 \pm 0.04)\%$. The trigger efficiency $\varepsilon_{\text{trig}}$ is 100% with an accuracy of better than 0.1% [20]. The integrated luminosity is determined to be $108.49 \pm 0.02 \pm 0.75$ pb^{-1} , where the first uncertainty is statistical and the second one is systematic, which will be discussed in Section 4.3.

4.3 Systematic uncertainty

Sources of systematic uncertainty include the requirements on track angles (θ , $\Delta\theta$, $\Delta\phi$) and the deposited

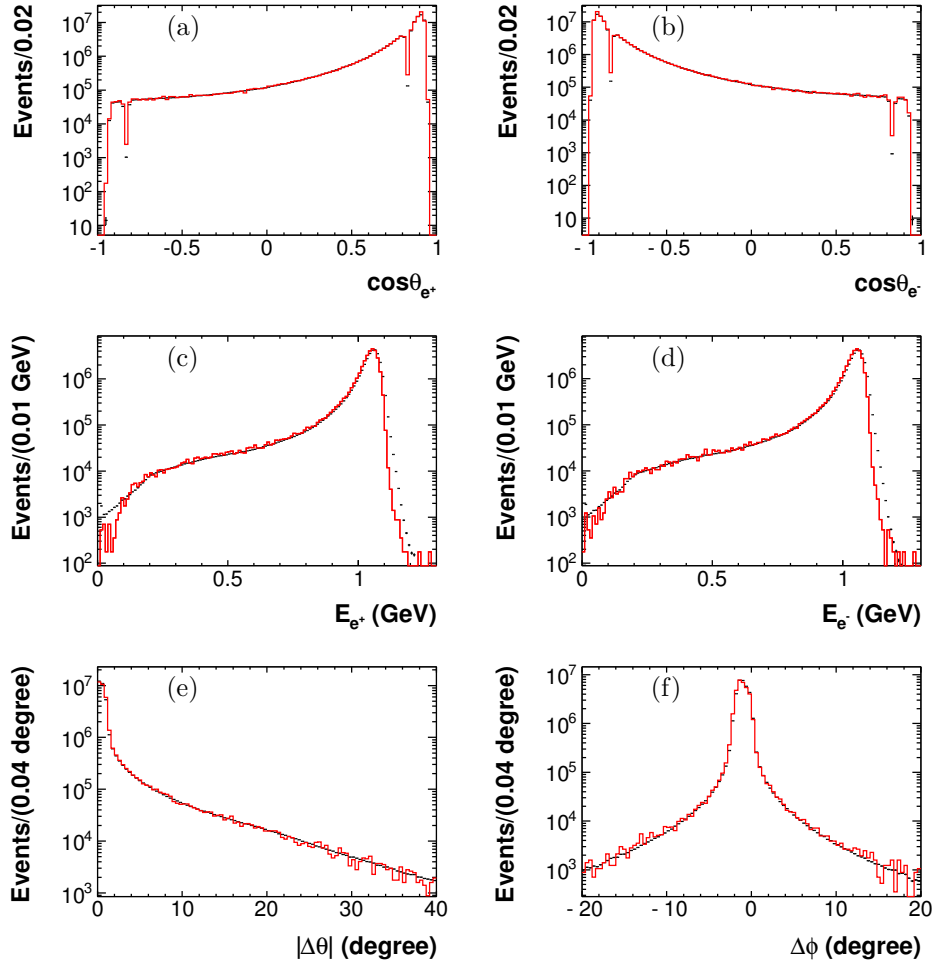


Fig. 1. Distributions of $\cos\theta$ of (a) e^+ and (b) e^- , deposited energy in the EMC of (c) e^+ and (d) e^- , (e) $|\Delta\theta|$ and (f) $\Delta\phi$ (measured in the laboratory frame of reference). The dots with error bars are for data, while the solid line indicates signal MC simulation.

energy in the EMC, the tracking efficiency, beam energy, MC statistics, trigger efficiency, and the MC generator.

To estimate the systematic uncertainties associated with the related angular requirements, the same selection criteria with alternative quantities were performed, individually, and the resultant (largest) difference with respect to the nominal result taken as the systematic uncertainty: $|\cos\theta| < 0.8$ was changed to $|\cos\theta| < 0.75$, resulting in a relative difference to the nominal result of 0.06%; $|\Delta\theta| < 10.0^\circ$ was changed to 8.0° or 15.0° , and the systematic uncertainty estimated to be 0.02%; $|\Delta\phi| < 5.0^\circ$ was changed to 4.0° or 10.0° , and the associated systematic uncertainty is 0.04%.

The uncertainty associated with the requirement on the deposited energy in the EMC is determined by comparing the detection efficiency between data and MC simulation. The data and MC samples were selected using the selection criteria listed in Section 4.1 except for the deposited energy requirement on the elec-

tron/positron. The efficiency is determined by the ratio between the numbers of events with and without the deposited energy requirement. The difference in the detection efficiency between data and signal MC simulation is 0.19% and 0.13% for electrons and positrons, respectively. The sum, 0.32%, is taken as the systematic uncertainty.

For the uncertainty associated with the tracking efficiency, it has been well studied in Ref. [21] by selecting a control sample of Bhabha events with the EMC information only. It was found that the difference between data and MC simulation is 0.41%, which is taken as the systematic uncertainty.

To estimate the systematic uncertainty associated with the beam energy, the luminosity is recalculated with the updated cross section and detection efficiency at the alternative center-of-mass energy of the measured value in Section 5. The difference from the nominal luminosity, 0.18%, is taken as the systematic uncertainty.

The uncertainty from MC statistics is 0.21% and from trigger efficiency is 0.1% [20]. The uncertainty due to the Babayaga generator is given as 0.5% [15].

All individual systematic uncertainties are summarized in Table 1. Assuming the individual uncertainties to be independent, the total systematic uncertainty is calculated by adding them quadratically and found to be 0.78%.

Table 1. Summary of the systematic uncertainties.

source	relative uncertainty(%)
$ \cos\theta < 0.8$	0.06
$ \Delta\theta < 10.0^\circ$	0.02
$ \Delta\phi < 5.0^\circ$	0.04
deposited energy requirement	0.32
tracking efficiency	0.41
beam energy	0.18
MC statistics	0.21
trigger efficiency	0.10
generator	0.50
total	0.78

4.4 Cross check

As a cross check, an alternative luminosity measurement using $e^+e^- \rightarrow \gamma\gamma$ events was performed. To select $e^+e^- \rightarrow \gamma\gamma$ events, candidate events must have two energetic clusters in the EMC. For each cluster, the polar angle was required to satisfy $|\cos\theta| < 0.8$ and the deposited energy E must be in region $0.7 \times E_{\text{beam}} < E < 1.15 \times E_{\text{beam}}$. To select clusters that are back-to-back, $|\Delta\phi| < 2.5^\circ$ (defined in Section 4.1) was required. In addition, there should be no good charged tracks satisfying $|V_z| < 10.0$ cm and $V_r < 1.0$ cm. With the selected $e^+e^- \rightarrow \gamma\gamma$ events, the integrated luminosity is determined to be 107.91 ± 0.05 pb⁻¹ (statistical only), which is in good agreement with the result obtained using large-angle Bhabha scattering events.

5 Measurement of the center-of-mass energy

5.1 Event selection

To select $e^+e^- \rightarrow (\gamma)\mu^+\mu^-$ candidates, we require exactly two good tracks with opposite charge satisfying $|V_z| < 10.0$ cm, $V_r < 1.0$ cm and $|\cos\theta| < 0.8$. To remove Bhabha events, the ratio of the deposited energy in the EMC and the momentum of a charged track, E/pc , was required to be less than 0.4. The two tracks should be back-to-back, with the $\Delta\theta$ and $\Delta\phi$ (defined in Section 4.1) satisfying $|\Delta\theta| < 10.0^\circ$ and $|\Delta\phi| < 5.0^\circ$. To further suppress background from cosmic rays, $|\Delta T| = |t_1 - t_2| < 1.5$ ns was required, where $t_{1/2}$ is the time of flight of the two charged tracks recorded by the TOF. Figure 2 shows

the comparisons between data and MC simulation, where the solid line is signal MC and the shaded histogram represents the simulation of background $e^+e^- \rightarrow q\bar{q}$.

With the above requirements, 1,472,195 events were selected in data with an estimated background level of about 1.8%. The small bumps visible in Figs. 2 (g) and (h) at about 0.93 GeV/ c mainly come from the $e^+e^- \rightarrow K^+K^-$ process. The peak at about 1.07 GeV/ c mainly consists of events from the processes $e^+e^- \rightarrow \pi^+\pi^-$ and $e^+e^- \rightarrow \pi^+\pi^-\gamma$.

5.2 Center-of-mass energy

Using the $e^+e^- \rightarrow (\gamma)\mu^+\mu^-$ events, the center-of-mass energy of the data set is determined with the method described in Ref. [12].

The center-of-mass energy can be determined with

$$M_{\text{CM}} = M_{\text{data}}(\mu^+\mu^-) - \Delta M, \quad (2)$$

where $M_{\text{data}}(\mu^+\mu^-)$ is the reconstructed $\mu^+\mu^-$ invariant mass of the selected $e^+e^- \rightarrow (\gamma)\mu^+\mu^-$ events, and ΔM is the correction for effects of ISR and FSR, which can be estimated using the $\mu^+\mu^-$ invariant mass of MC samples with ISR/FSR turned on ($M_{\text{MC, on}}(\mu^+\mu^-)$) and off ($M_{\text{MC, off}}(\mu^+\mu^-)$):

$$\Delta M = M_{\text{MC, on}}(\mu^+\mu^-) - M_{\text{MC, off}}(\mu^+\mu^-). \quad (3)$$

By fitting the $M_{\text{MC, on}}(\mu^+\mu^-)$ and $M_{\text{MC, off}}(\mu^+\mu^-)$ distributions of MC samples, the average of ΔM is determined to be -1.13 MeV/ c^2 , where $M_{\text{MC, on}} = 2124.60 \pm 0.04$ MeV/ c^2 , $M_{\text{MC, off}} = 2125.73 \pm 0.01$ MeV/ c^2 , and the errors are statistical only. The function fitted to $M_{\text{MC, on}}$ is a Gaussian plus a Crystal Ball function [22] with a common mean, and the function fitted to $M_{\text{MC, off}}$ is a double Gaussian function with a common mean. The fit results are shown in Fig. 3. To calculate ΔM (and M_{CM}) as a function of run number, $M_{\text{MC, off}}$ and $M_{\text{MC, on}}$ for each run are fitted with the above same functions.

For each run, $M_{\text{data}}(\mu^+\mu^-)$ was fitted in the range [2.0, 2.2] GeV/ c^2 . The signal is described by a Gaussian plus a Crystal Ball function with a common mean, while the background is ignored (about 1.1% in the fit range). As an example, the fit result for run 42030 is shown in Fig. 4.

M_{CM} was calculated with Eq. (2) and Eq. (3) for each run. The average of M_{CM} for the full data set is determined to be 2126.55 ± 0.03 MeV/ c^2 by fitting the M_{CM} of different runs with a constant. The M_{CM} distribution as a function of run number and the overall fit result are shown in Fig. 5, where 21 runs are excluded in the fit due to large statistical errors (less than 100 entries in the fit range). The M_{CM} values for individual runs are shown in Fig. 6 as a histogram, which can be fitted very well with a Gaussian function with the parameters $\mu = 2126.55 \pm 0.03$ MeV/ c^2 and $\sigma = 0.98 \pm 0.03$ MeV/ c^2 .

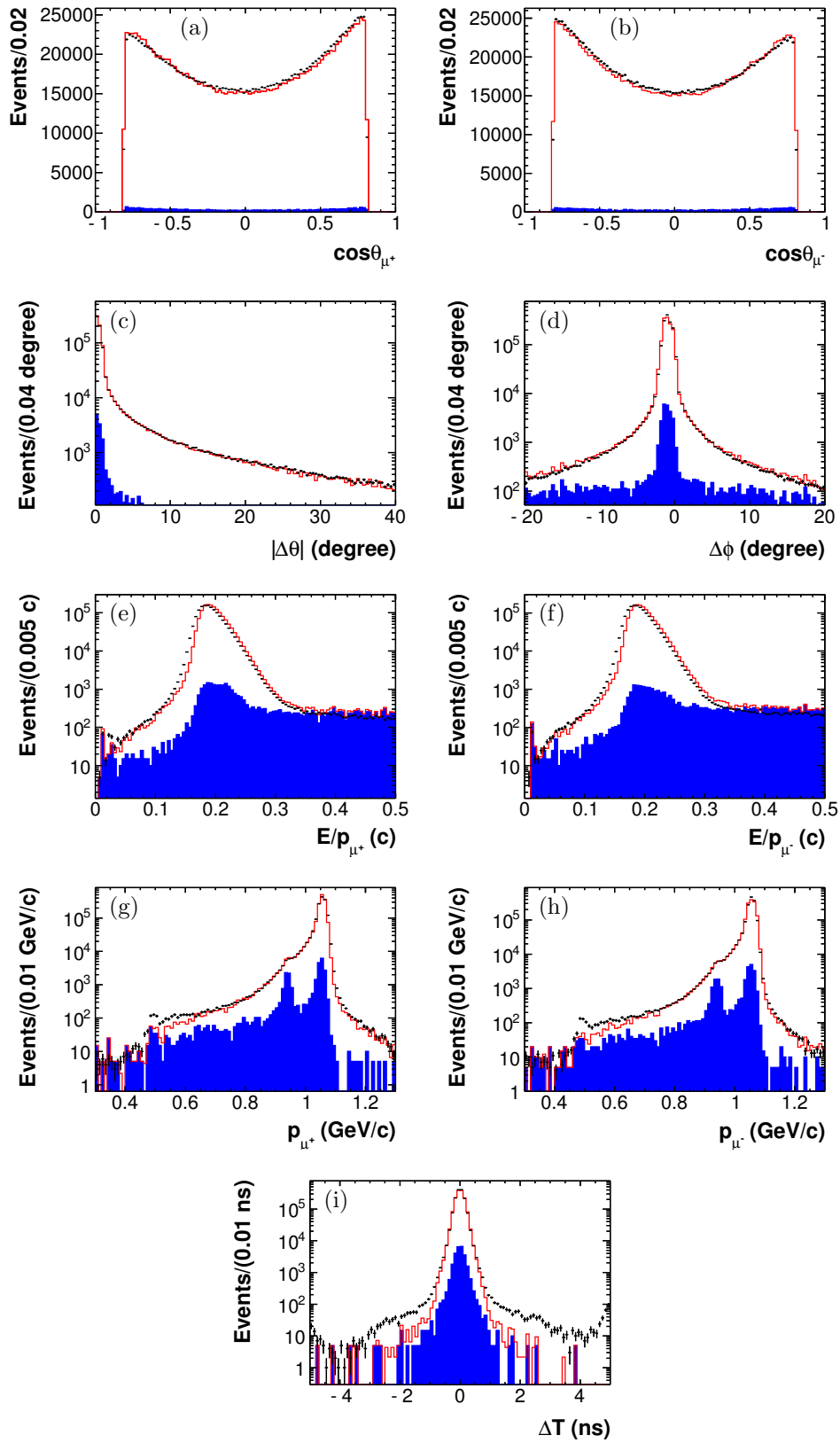


Fig. 2. Distributions of $\cos\theta$ of (a) μ^+ and (b) μ^- , (c) $|\Delta\theta|$, and (d) $\Delta\phi$ (measured in the laboratory frame of reference), E/p distributions of (e) μ^+ and (f) μ^- , momentum distributions of (g) μ^+ and (h) μ^- , and (i) ΔT distribution. The dots with error bars represent the data, the solid line indicates signal MC simulation, and the shaded histogram represents the MC simulation of $e^+e^- \rightarrow q\bar{q}$.

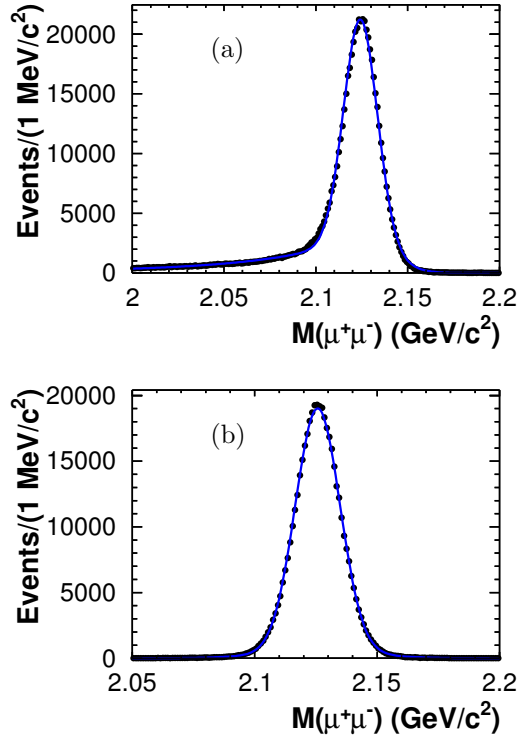


Fig. 3. Fit to $M(\mu^+\mu^-)$ of MC sample (a) with and (b) without ISR/FSR.

5.3 Systematic uncertainty

As shown in Section 5.2, $M_{MC, off} = 2125.73 \pm 0.01$ MeV/ c^2 is 0.73 MeV/ c^2 higher than the input value (2125 MeV/ c^2). This difference is taken as the systematic uncertainty.

The uncertainty of the momentum measurement of two muon tracks has been studied using $e^+e^- \rightarrow \gamma_{ISR}J/\psi, J/\psi \rightarrow \mu^+\mu^-$ in Ref. [12], and is estimated to be 0.011%.

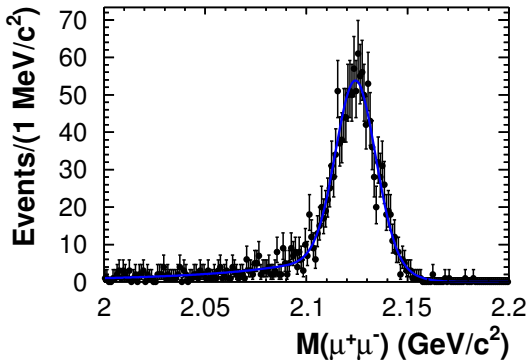


Fig. 4. Fit to $M(\mu^+\mu^-)$ for run 42030. Dots with error bars are data, while the solid line is the fit result.

To estimate the uncertainty from the fit to the invariant mass of $\mu^+\mu^-$, the signal shape and fit range

were varied and M_{CM} re-calculated. The difference to the nominal result is taken as the systematic uncertainty. The systematic uncertainty from signal shape is estimated to be 0.08 MeV/ c^2 by replacing the Crystal Ball function in the signal shape with the GaussExp function [23]. The systematic uncertainty from fit range is estimated to be 0.13 MeV/ c^2 by varying the fit range to [2.00, 2.14] GeV/ c^2 and [2.10, 2.20] GeV/ c^2 , respectively.

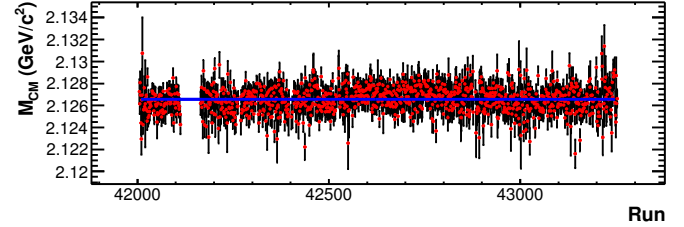


Fig. 5. Distribution of M_{CM} for individual runs. The solid line is the average fit.

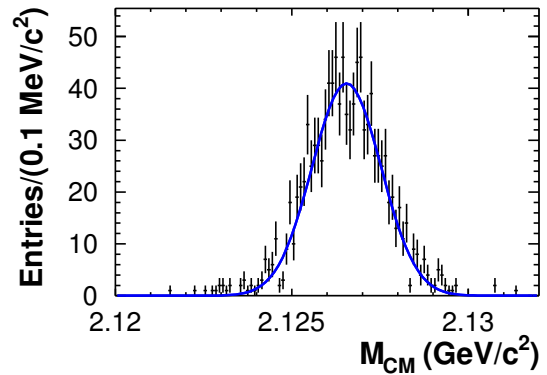


Fig. 6. Histogram of M_{CM} for individual runs. The solid line is a Gaussian function.

To estimate the uncertainty from the fit to the M_{CM} distribution, fits in different ranges of the run number were carried out. The resultant maximum difference with respect to the nominal value, 0.34 MeV/ c^2 , is taken as the uncertainty.

Assuming all of the above uncertainties are independent, the total systematic uncertainty is calculated to be 0.85 MeV/ c^2 by adding the individual items in quadrature.

6 Summary

The integrated luminosity of the data taken at 2.125 GeV in 2015 with the BESIII detector is measured to be $108.49 \pm 0.02 \pm 0.85$ pb $^{-1}$ using large-angle Bhabha events. A cross check with $e^+e^- \rightarrow \gamma\gamma$ events was performed and the result is 107.91 ± 0.05 pb $^{-1}$ (statistical

only), which is in good agreement with the nominal result within the uncertainties. With $e^+e^- \rightarrow (\gamma)\mu^+\mu^-$ events, the center-of-mass energy of the data set is measured to be $2126.55 \pm 0.03 \pm 0.85$ MeV. The results in this measurement are important input for physics stud-

ies, e.g., studies of decays of the $Y(2175)$.

The BESIII collaboration would like to thank the staff of BEPCII and the IHEP computing center for their dedicated support.

References

- 1 C. Patrignani et al (Particle Data Group), *Chin. Phys. C*, **40**: 100001 (2016)
- 2 B. Aubert et al (BaBar Collaboration), *Phys. Rev. D*, **74**: 091103 (2006)
- 3 B. Aubert et al (BaBar Collaboration), *Phys. Rev. D*, **76**: 012008 (2007)
- 4 M. Ablikim et al (BES Collaboration), *Phys. Rev. Lett.*, **100**: 102003 (2008)
- 5 C. P. Shen et al (Belle Collaboration), *Phys. Rev. D*, **80**: 031101 (2009)
- 6 M. Ablikim et al (BESIII Collaboration), *Phys. Rev. D*, **91**: 052017 (2015)
- 7 G. J. Ding and M. L. Yan, *Phys. Lett. B*, **650**: 390 (2007)
- 8 G. J. Ding and M. L. Yan, *Phys. Lett. B*, **657**: 49 (2007)
- 9 Z. G. Wang, *Nucl. Phys. A*, **791**: 106 (2007)
- 10 E. Klempt and A. Zaitsev, *Phys. Rep.*, **454**: 1 (2007)
- 11 M. Ablikim et al (BESIII Collaboration), *Nucl. Instrum. Methods Phys. Res., Sect. A*, **614**: 345 (2010)
- 12 M. Ablikim et al (BESIII Collaboration), *Chin. Phys. C*, **40**: 063001 (2016)
- 13 S. Agostinelli et al (GEANT4 Collaboration), *Nucl. Instrum. Methods Phys. Res., Sect. A*, **506**: 250 (2003)
- 14 J. Allison et al, *IEEE Trans. Nucl. Sci.*, **53**: 270 (2006)
- 15 G. Balossini, C. M. Carloni Calame, G. Montagna, O. Nicrossini and F. Piccinini, *Nucl. Phys. B*, **758**: 227 (2006)
- 16 R. G. Ping, *Chin. Phys. C*, **32**: 599 (2008)
- 17 D. J. Lange, *Nucl. Meth. A*, **462**: 152 (2001)
- 18 B. Andersson, *The Lund Model*, (Cambridge University Press, 1998)
- 19 B. Andersson, H. Hu, hep-ph/9910285 (1999)
- 20 N. Berger, K. Zhu et al, *Chin. Phys. C*, **34**: 1779 (2010)
- 21 M. Ablikim et al (BESIII Collaboration), *Chin. Phys. C*, **41**: 063001 (2017)
- 22 T. Skwarnicki et al, Report No. DESY F31-86-02 (1986) (unpublished)
- 23 S. Das, arXiv:1603.08591 [hep-ex]